Shi *et al. Discover Oncology* (2025) 16:1073
https://doi.org/10.1007/s12672-025-02934-0

Discover Oncology

ANALYSIS Open Access

Comprehensive analysis of SELPLG as a potential immunotherapy target and prognostic biomarker in oncology

Ranran Shi[1,2], Ling Ran[1,2], Beibei Li[3], Yuan Tian[1,2], Wei Guo[1], Shaoju Jin[1,3*] and Wenshan Zhao[3*]

*Correspondence:
Shaoju Jin
shaojujin@163.com
Wenshan Zhao
zhaowsh07@zzu.edu.cn
[1]Department of Basic Medical Sciences, Luohe Medical College, Luohe 462000, China
[2]Henan Province Engineering & Technology Research Center of Foods for Special Medical Purpose, Luohe Medical College, Luohe 462000, China
[3]School of Life Sciences, Zhengzhou University, Zhengzhou 450001, China

Abstract

Background *SELPLG*, which encodes P-selectin glycoprotein ligand-1, has emerged as a potential oncological target. A comprehensive understanding of its expression patterns across various cancer types and stages is crucial for elucidating its prognostic, therapeutic, and immunological roles.

Methods We conducted an extensive bioinformatics analysis using multiple computational tools. TIMER2 was employed to quantify *SELPLG* mRNA expression in both tumor and normal tissues across diverse cancer types. Expression differences were further analyzed across clinical TNM stages and T stages. To investigate *SELPLG* expression at cellular and subcellular levels, we integrated genetic localization and single-cell sequencing data. A pan-cancer mutational landscape analysis was performed using Sangerbox 3.0. The prognostic significance of *SELPLG* expression was assessed using Cox proportional hazards regression models. Gene set enrichment analysis (GSEA) identified *SELPLG*-associated signaling pathways, while correlation analyses examined its relationship with immune cell infiltration.

Results *SELPLG* was significantly upregulated in multiple tumor types, including breast (BRCA), cholangiocarcinoma (CHOL), esophageal (ESCA), head and neck (HNSC), kidney chromophobe (KICH), kidney renal papillary carcinoma (KIRP), stomach (STAD), and thyroid (THCA) cancers. Conversely, it was downregulated in lung adenocarcinoma (LUAD), colon (COAD), lung squamous cell carcinoma (LUSC), and bladder (BLCA) cancers. Differential expression analyses reinforced these findings across various cancer types and stages. Genetic localization studies revealed predominant *SELPLG* expression in lymphoid and myeloid cells, while single-cell sequencing data indicated enrichment in immune cell populations. The mutational landscape analysis identified frequent missense mutations across cancers. Prognostic analyses confirmed significant associations between *SELPLG* expression and patient outcomes. GSEA indicated *SELPLG*'s involvement in immune-related pathways, and correlation analyses established a positive association between *SELPLG* expression and immunomodulatory factors.

Conclusions This comprehensive study supports *SELPLG* as a promising prognostic, therapeutic, and immunological biomarker in cancer. Our findings underscore its role

in tumor progression, immune response modulation, and potential as a therapeutic target.

Keywords *SELPLG*, Prognosis, Immune infiltration, Tumor immunotherapy, Therapeutic targets

1 Introduction

Cancer remains a major global health burden, with both incidence and mortality rates continuing to rise. In recent years, immunotherapy has revolutionized cancer treatment by shifting the therapeutic paradigm away from traditional approaches such as chemotherapy, radiotherapy, and surgery. Among these, immune checkpoint blockade (ICB), particularly the inhibition of PD-1/PD-L1, has emerged as a powerful strategy that enhances $CD8^+$ T cell-mediated cytotoxicity against tumors. However, a substantial proportion of patients do not respond to current immunotherapies, highlighting the urgent need to identify novel immune-related therapeutic targets [1].

P-selectin glycoprotein ligand-1 (PSGL-1), encoded by the *SELPLG* gene, has garnered interest for its roles in tumorigenesis and immune regulation. PSGL-1 is highly expressed in various cancer cell lines, including small cell lung cancer (SCLC), alveolar carcinoma, multiple myeloma (MM), and metastatic prostate cancer [2]. Through interactions with its ligands, P-selectin and E-selectin, PSGL-1 facilitates tumor metastasis [3]. In murine MM model, PSGL-1 promotes bone marrow homing and proliferation via P-selectin-mediated adhesion, while *SELPLG* knockout suppresses tumor growth. Similar pro-metastatic roles have been reported in bone-metastatic prostate and lung cancer [4–6]. In non-small cell lung cancer (NSCLC), PSGL-1 interacted with activated platelet P-selectin enhances metastatic potential [6, 7]. Clinically, elevated PSGL-1 correlates with advanced MM stages. Beyond metastasis, PSGL-1 has been implicated in therapy resistance. In MM, it activates ERK1/2 signaling and MYC expression through macrophage interaction, leading to increased proliferation and drug resistance [8]. Notably, dual blockade of PSGL-1 and P-selectin enhances bortezomib sensitivity in preclinical models [9]. In acute myeloid leukemia (AML), PSGL-1 promotes chemoresistance via E-selectin and *SELPLG* deletion enhances chemotherapy efficacy [10]. These findings collectively support a critical role for PSGL-1 in cancer progression, metastasis, and chemoresistance.

In addition to its tumor-intrinsic functions, PSGL-1 exhibits immunosuppressive role. $SELPLG^{-/-}$ mice develop spontaneous autoimmune disorders affecting the skin, lungs, and kidneys [11], and in lupus-prone mice, its deficiency induces glomerulonephritis, scleroderma, ulcerative colitis, and experimental autoimmune encephalomyelitis [12–14]. In the tumor microenvironment, PSGL-1 is upregulated on migrating T cells, where it dampens TCR signaling, inhibits IL-2 survival pathways, and promotes exhaustion [15]. $SELPLG^{-/-}$ mice exhibit stronger effector T cell responses and improved control of chronic infections and melanoma [16]. In B16 melanoma models, PSGL-1 blockade enhanced $CD4^+$ and $CD8^+$ T cell infiltration and cytotoxicity, reduced regulatory T cells (Tregs), and delayed tumor progression. PSGL-1 also influences other immune cell subsets. In the thymus, *SELPLG* deficiency results in reduced Treg development, while in dendritic cells (DCs), PSGL-1 engagement promotes immunosuppressive phenotypes that facilitate Treg induction and suppress effector T cell proliferation [17–19].

SELPLG$^{-/-}$ DCs exhibited enhanced immunogenicity, whereas PSGL-1 signaling in human monocyte-derived DCs promotes tolerance.

Despite mounting evidence of its oncogenic and immunoregulatory functions, a comprehensive pan-cancer characterization of *SELPLG* remains lacking. To address this gap, we conducted a systematic investigation to profile *SELPLG* expression, prognostic significance, immune associations, and potential as a therapeutic target across multiple cancer types.

2 Methods

2.1 Data collection and preprocessing

The TCGA Pan-Cancer dataset (PANCAN, $N = 10{,}535$ samples, $G = 60{,}499$ genes) was downloaded from the UCSC Xena Browser (https://xenabrowser.net/), provides unif ormly normalized RNA-seq data. To ensure robust analysis, we excluded cancer types with fewer than three samples in any of the sample categories (Solid Tissue Normal, Primary Tumor, or Primary Blood Derived Cancer). Subsequently, we retrieved the expression data for the *SELPLG* gene across multiple samples. *SELPLG* expression data were filtered from solid tissue normal, peripheral blood, and primary tumor samples, and transformed using $\log_2(x + 0.001)$. We accessed the Human Protein Atlas (HPA) to examine *SELPLG* protein expression across cancers, enabling insight into its tumor-specific profiles. Somatic mutations were analyzed using the Catalogue of Somatic Mutations in Cancer (COSMIC v96). Mutation hotspots and functional impacts were annotated using the maftools R package.

2.2 Pan-cancer mutational landscape of *SELPLG*

The Simple Nucleotide Variation dataset at level 4 was obtained from TCGA samples processed via MuTect2 software through the GDC (https://portal.gdc.cancer.gov/) [20]. Mutation data of the samples was integrated, and protein structural domain information was acquired from the R software package maftools [21]. To ensure high-confidence calls, mutations with a variant allele frequency (VAF) < 5% or read depth < 10 were filtered out. Mutation landscapes were visualized using maftools, and recurrent mutations were cross-referenced with COSMIC annotations to prioritize clinically relevant variants. The STAD mutation dataset includes 414 samples with detected mutations, of which 365 samples (88.2%) are visualized. The COAD mutation dataset consists of 288 samples with detected mutations, of which 275 samples (95.5%) are visualized. Gene mutation frequencies within each sample group were evaluated.

2.3 Survival analysis of *SELPLG*

We utilized a high-quality TCGA prognostic dataset from a previously published Cell study [22]. Samples with follow-up times less than 30 days were excluded, and a logarithmic transformation of $\log_2(x + 0.001)$ was applied to each expression value. Cancer types with fewer than 10 samples were removed, resulting in expression data and overall survival data for 39 cohorts (TCGA-GBM, TCGA-GBMLGG, TCGA-LGG, TCGA-CESC, TCGA-LUAD, TCGA-LAML, TCGA-BRCA, TCGA-ESCA, TCGA-STES, TCGA-SARC, TCGA-KIRP, TCGA-KIPAN, TCGA-PRAD, TCGA-STAD, TCGA-HNSC, TCGA-KIRC, TCGA-COAD, TCGA-COADREAD, TCGA-LUSC, TCGA-THYM, TCGA-LIHC, TCGA-THCA, TCGA-MESO, TCGA-READ, TCGA-SKCM-M,

TCGA-SKCM, TCGA-OV, TCGA-TGCT, TCGA-PAAD, TCGA-UCEC, TCGA-PCPG, TCGA-SKCM-P, TCGA-UVM, TCGA-UCS, TCGA-BLCA, TCGA-ACC, TCGA-KICH, TCGA-CHOL, TCGA-DLBC).

The R package maxstat was used to determine the optimal *SELPLG* cutoff (1.9749), ensuring a minimum group size greater than 25% and maximum group sample size below 75%. Kaplan-Meier survival curves were generated using survfit, and the log-rank test was applied to evaluate significance.

2.4 Gene set enrichment analysis (GSEA) of *SELPLG*

To explore the biological pathways and processes associated with *SELPLG* expression, we performed Gene Set Enrichment Analysis (GSEA) using the Molecular Signatures Database (MSigDB) hallmark sets. The analysis included hallmark gene sets, Gene Ontology (GO) terms, and KEGG pathways. GSEA was conducted on pan-cancer cohorts to identify pathways significantly enriched in high versus low *SELPLG* expression groups. The results were visualized using enrichment plots and heatmaps to illustrate the correlation between *SELPLG* expression and immune-related pathways. We utilized the TCGA cohort to identify genes associated with *SELPLG* and conducted correlation analysis. Hallmark gene sets from the Molecular Signatures Database (MSigDB v7.5.1) were used. GSEA was performed using default parameters (1,000 permutations). Pathways with FDR < 0.25 and |NES| > 1.5 were deemed significant. Genes ranked by Pearson correlation coefficient with *SELPLG* expression ($P < 0.05$). Enrichment plots and heatmaps were generated using the BEST tool (https://rookieutopia.com/).

2.5 Quantification of immune cell infiltration on *SELPLG* expression levels

Immune cell infiltration scores were obtained from TIMER2.0 (http://timer.cistrome.org/) and a published TCGA immune deconvolution study. Patients were stratified by median *SELPLG* expression to compare infiltration levels between groups.

2.6 Analysis of *SELPLG* correlation with Immunomodulatory genes

Additionally, *SELPLG* expression was correlated with 60 immunomodulatory genes from key immune checkpoint pathways [23]. After filtering out samples from Primary Blood Derived Cancer - Peripheral Blood and Primary Tumor, excluding normal samples, we applied a logarithmic transformation of $\log_2(x + 0.001)$ to each expression value. Following this, we calculated the Pearson correlation between *SELPLG* and marker genes from five immune pathways.

2.7 Statistical analysis

Statistical analysis was performed using ggplot2 (v3.3.2) in the R program v4.0.3. Statistical significance between groups was determined using a two-tailed Student's t-test or one-way ANOVA. A significance level of $P < 0.05$ was considered statistically significant.

3 Results

3.1 Expression of *SELPLG* across cancer types and stages

The role of *SELPLG* in cancer was analyzed using pan-cancer samples from TCGA database. The research design and workflow diagram used in this study is shown in Fig. 1. *SELPLG* RNA expression across various tumor and normal tissues was assessed using

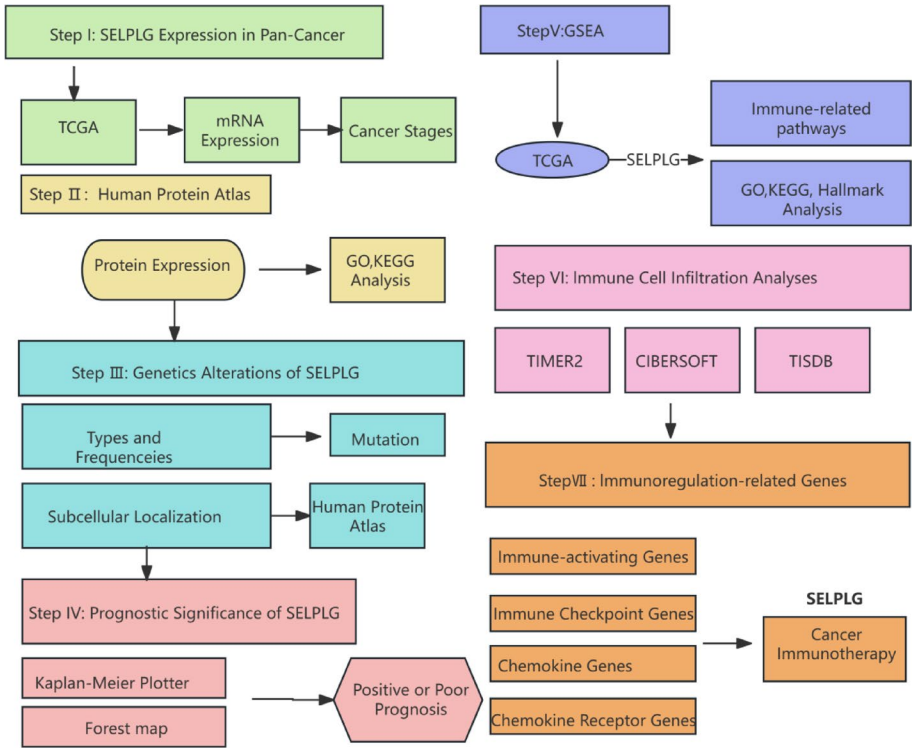

Fig. 1 Workflow diagram of the study design

TIMER2. The analysis revealed significant upregulation of *SELPLG* in eight tumor types (BRCA, CHOL, ESCA, HNSC, KIPC, KIRP, STAD, and THCA), whereas notable downregulation was observed in LUAD, COAD, LUSC, and BLCA (Fig. 2A). Differential expression between tumor and normal samples was further analyzed using the Wilcoxon rank-sum and signed-rank tests in R. Significantly elevated expression was found in ten tumor types (BRCA, ESCA, STES, KIRP, KIPAN, STAD, HNSC, KIRC, THCA, and CHOL), while downregulation was observed in LUAD, COAD, COADREAD, LUSC, and BLCA (Fig. 2B). To evaluate *SELPLG* expression across clinical TNM stages, pairwise comparisons were performed using the unpaired Student's t-test and ANOVA. Significant stage-related differences were detected in STES, KIPAN, STAD, THYM, THCA, PAAD, BLCA, and KICH (Fig. 2C). Similarly, significant variation across T stages was observed in LUAD, STES, KIPAN, STAD, PRAD, HNSC, BLCA, and KICH (Fig. 2D).

3.2 Genetic localization and single-cell expression of *SELPLG*

SELPLG RNA expression across various cell types was profiled using data from the Human Protein Atlas (HPA). The gene was found to be largely absent in tumor cells, but selectively expressed in lymphoid and myeloid lineages (Fig. 3A). Subcellular localization analysis demonstrated that *SELPLG* was primarily localized within vesicles in HEL, JURKAT, and U2OS cell lines, with additional localization in the nucleus, microtubules, and endoplasmic reticulum (Fig. 3B–C). Elevated *SELPLG* expression was also detected in NSCLC and colorectal cancer tissues (Fig. 3D). Single-cell sequencing further confirmed strong enrichment of *SELPLG* in immune cell subsets, especially dendritic cells, monocytes, NK cells, T cells, and macrophages (Fig. 3E–F).

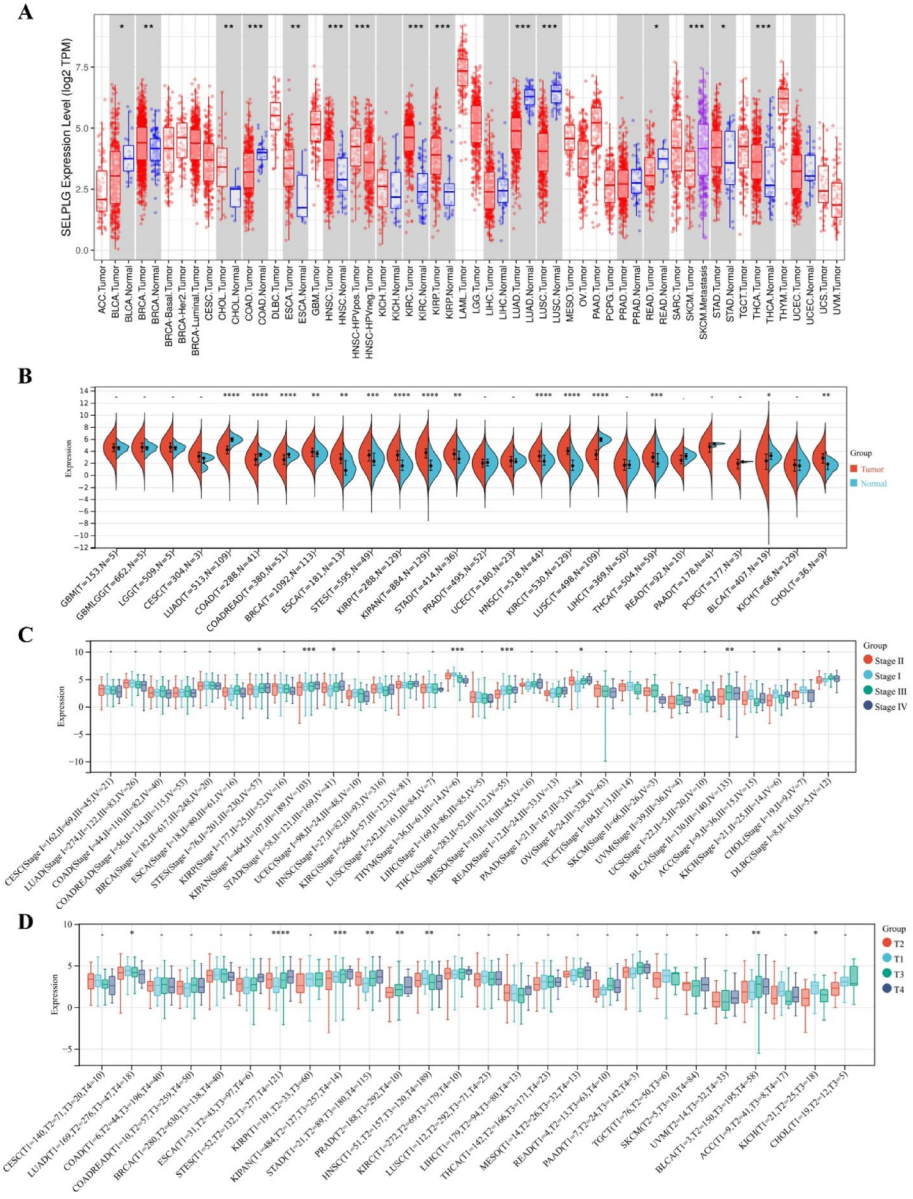

Fig. 2 The expression patterns of *SELPLG* across different cancer types and clinical stages based on analyses conducted using TIMER2 and other computational tools. **A** Expression analysis of *SELPLG* across various cancers with or without paracancer generated from TIMER (https://cistrome.shinyapps.io/timer/). **B** Expression analysis of *SELPLG* across various cancers with or without paracancer generated from other analyses. **C** Analysis of *SELPLG* expression across TNM stage samples. **D** Differential expression analysis of *SELPLG* across clinical T stage samples

3.3 Association between *SELPLG* expression and mutational landscape

The expression profile and mutational landscape of *SELPLG* across various cancer types were analyzed using Sangerbox 3.0 (http://sangerbox.com/home.html). Missense mutations were the predominant type across most cancer types (Fig. 4A). To explore mutation patterns in relation to *SELPLG* expression, samples were stratified into high- and low-expression groups in STAD and COAD. In STAD, frequent mutations included TTN, TP53, LRP1B, and SYNE1, predominantly of the missense type (Fig. 4B). In contrast, in COAD showed frequent mutations in APC, TTN, and MUC16, with a high proportion of nonsense mutations in APC (Fig. 4C). Correlation analysis between *SELPLG* expression and tumor mutational burden (TMB) revealed cancer-specific trends. A negative

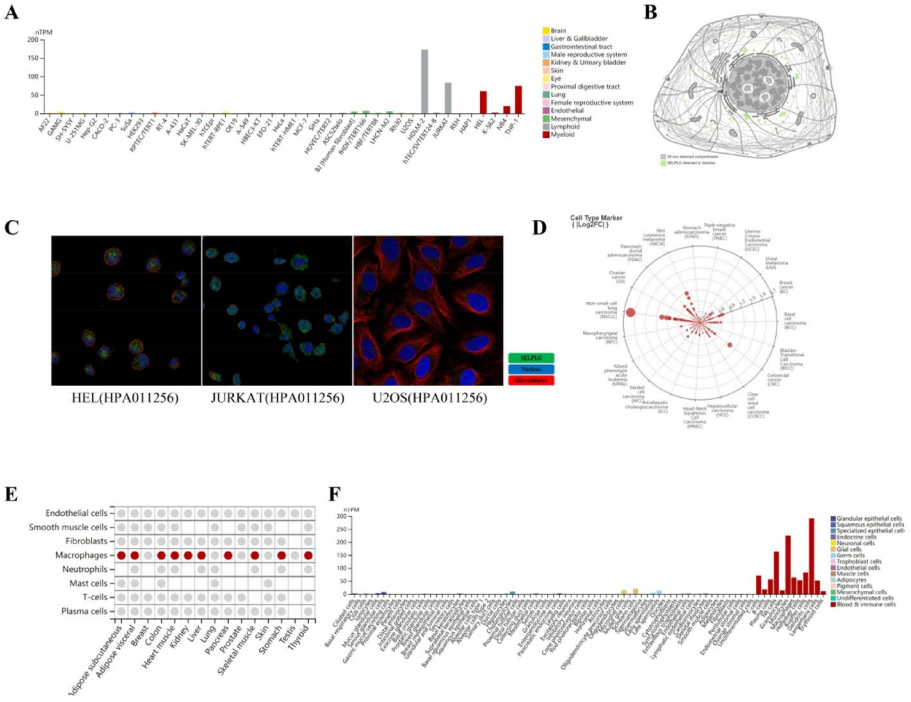

Fig. 3 Comprehensive analysis of *SELPLG* expression and subcellular localization across various cell types and conditions. **A***SELPLG* expression profiles in diverse tumor cell lines, as derived from The Human Protein Atlas. This panel displays differential expression levels across multiple tumor-derived cell lines. **B** Schematic representation of *SELPLG* subcellular localization, highlighting its predominant distribution within key cellular compartments. **C** Immunofluorescence staining of *SELPLG* localization in HEL, JURKAT, and U2OS cell lines. Images obtained from The Human Protein Atlas illustrate specific subcellular structures where *SELPLG* is detected. **D** Relative *SELPLG* expression across various cell types, including endothelial cells, smooth muscle cells, fibroblasts, and macrophages. **E** Comparative enrichment of *SELPLG* expression among core cell populations, indicating the cell types with the highest and lowest levels of expression. **F** Single-cell RNA sequencing analysis of *SELPLG* expression across immune cell subsets. Expression variability is shown across T cells, plasma cells, and other immune cell types

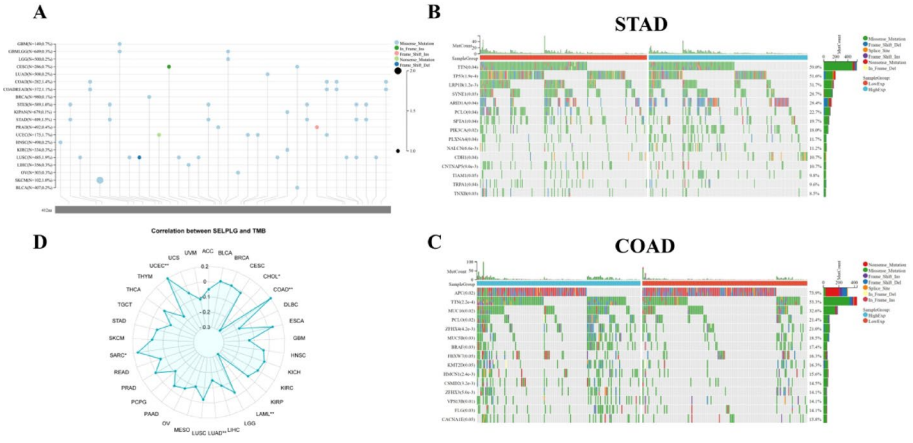

Fig. 4 Comprehensive analysis of the mutational landscape associated with *SELPLG* across different cancer types. **A** Pan-cancer analysis of *SELPLG* gene mutation types in various types of cancers. The mutation types and mutant genes of the high- and low-expression groups of *SELPLG* in STAD (**B**) and COAD (**C**) were analyzed. **D** Correlation of *SELPLG* expression with TMB

correlation was observed in CHOL and LAML, while UCEC, COAD, and SARC showed a significant positive correlation (Fig. 4D). These findings suggest that *SELPLG* may play a differential role in shaping the mutational landscape of tumors and could serve as a potential biomarker for predicting TMB levels in distinct cancer types.

3.4 The prognostic significance of *SELPLG* expression across cancer types

The prognostic value of *SELPLG* across cancers was assessed using the Cox proportional hazards model with log-rank tests. High *SELPLG* expression was associated with poorer overall survival (OS) in LAML, KIPAN, and UVM, whereas low expression predicted worse outcomes in CESC, SARC, HNSC, and SKCM (including metastasis subgroup) (Fig. 5A). In disease-specific survival (DSS) analysis, high *SELPLG* expression correlated with poorer prognosis in GBMLGG, LGG, KIPAN, TGCT, and UVM. Conversely, low expression was associated with unfavorable outcomes in CESC, HNSC, THCA, and SKCM (Fig. 5B). For disease-free interval (DFI), low *SELPLG* expression predicted worse outcomes in LIHC and BLCA (Fig. 5C). In progression-free interval (PFI), high *SELPLG* expression was linked to poor prognosis in GBMLGG, LGG, KIPAN, and PRAD,

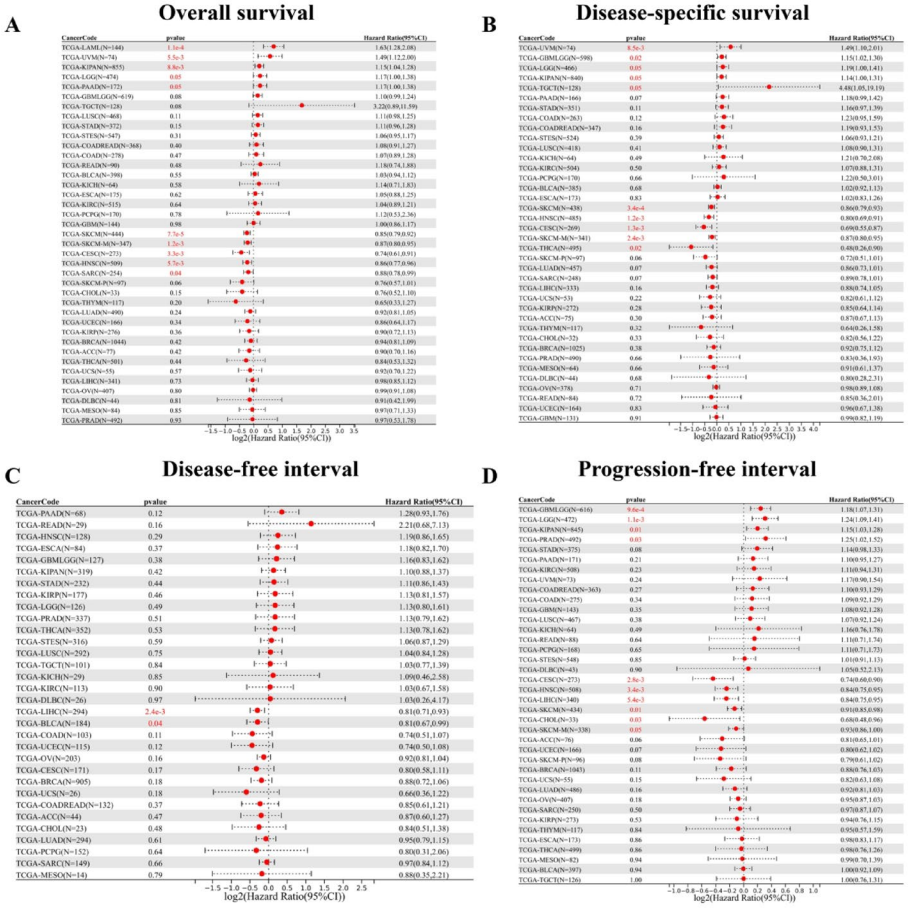

Fig. 5 Univariate Cox regression analyses assessing the prognostic impact of *SELPLG* expression across different types of cancer. **A** The association between *SELPLG* expression levels and overall survival (OS) rates across various cancer types using the Cox regression model. **B** The univariate Cox regression analyses evaluating *SELPLG* in terms of disease-specific survival (DSS) rates across 33 types of cancer in the TCGA database. **C** The outcomes of univariate Cox regression analyses examining *SELPLG* in relation to disease-free interval (DFI) rates in diverse cancer types. **D** The results of univariate Cox regression analyses assessing *SELPLG* for progression-free interval (PFI) rates across various cancer types

whereas low expression indicated unfavorable outcomes in CESC, HNSC, LIHC, SKCM, and CHOL (Fig. 5D). Similar results were obtained from the Kaplan-Meier Plotter analysis (Fig. S1).

3.5 *SELPLG*-associated signaling pathways identified by gene set enrichment analysis (GSEA)

Gene Set Enrichment Analysis (GSEA) was conducted using the BEST (rookieutopia.com) platform to identify biological processes associated with *SELPLG*. This analysis encompassed Gene Ontology (GO), Kyoto Encyclopedia of Genes and Genomes (KEGG), and Hallmark gene sets, providing a comprehensive assessment of *SELPLG*-related pathways [24]. GO analysis revealed enrichment in immune-related processes, including T cell activation, adaptive immune response, antigen processing and presentation via MHC class II, and leukocyte proliferation (Fig. 6A). KEGG pathway analysis identified associations with immune pathways such as antigen processing and presentation, natural killer (NK) cell-mediated cytotoxicity, chemokine signaling, T cell receptor signaling, and B cell receptor signaling (Fig. 6B, D). Hallmark pathway analysis highlighted the involvement of *SELPLG* in key immune and inflammatory processes, including inflammatory response, IL-6/JAK-STAT3 signaling, interferon-gamma response, IL-2/STAT5 signaling, and TNF-α signaling via NF-κB (Fig. 6C). Additionally,

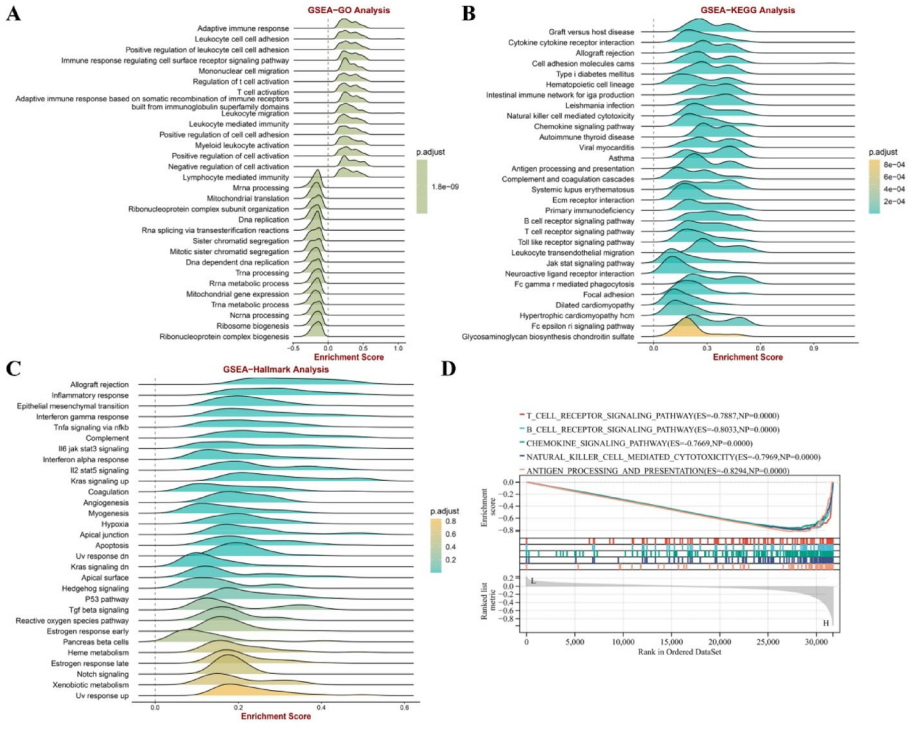

Fig. 6 Gene Set Enrichment Analysis (GSEA) of hallmark pathways associated with *SELPLG* expression in pan-cancer cohorts. **A** Gene ontology (GO) enrichment analysis of *SELPLG* with immune-related functions. This panel displays the results of GO enrichment analysis, highlighting the biological processes, molecular functions, and cellular components associated with *SELPLG* expression, particularly focusing on immune-related functions. The analysis was performed using the GSEA method on pan-cancer data. **B**, **D** Correlations of *SELPLG* with immune-related pathways revealed by KEGG pathway analysis. These panels illustrate the significant immune-related pathways correlated with *SELPLG* expression, as identified through KEGG pathway analysis. **C** Hallmark pathway enrichment analysis of *SELPLG*'s involvement in immune-related processes. The analysis was conducted using the GSEA method, and the results are visualized to show the normalized enrichment scores (NES) and false discovery rates (FDR) for each pathway

over-representation analysis (ORA) consistently supported these findings (Fig. S2–S3), reinforcing the pivotal role of *SELPLG* in immune regulation and inflammatory signaling. Collectively, these data underscore the potential involvement of *SELPLG* in immune modulation and inflammatory signaling pathways.

4 Immune cell infiltration analyses

To examine immune cell infiltration, six algorithms within TIMER2 were used. *SELPLG* expression showed positive correlations with $CD8^+$ T cells, $CD4^+$ T cells, B cells, macrophages, and Tregs, and negative correlations with myeloid-derived suppressor cells (MDSCs) (Fig. 7A–F). CIBERSORT further confirmed these trends, highlighting positive associations with Tregs, $CD8^+$ T cells, and both M1 and M2 macrophages, and

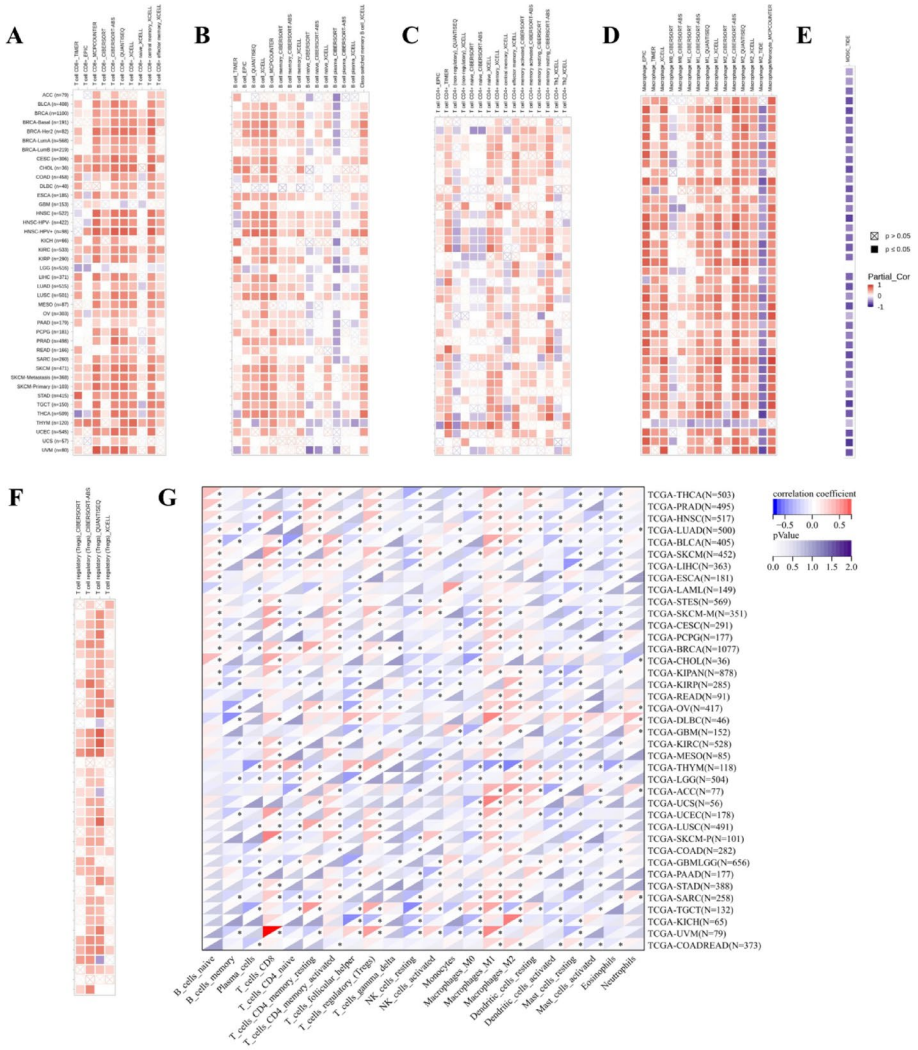

Fig. 7 Association between *SELPLG* expression and immune cell infiltration levels across TCGA tumors based on TIMER2.0 and CIBERSORT analyses. **A** The correlation between *SELPLG* and infiltration level of $CD8^+$ T cells using TIMER2 database. **B** The correlation between *SELPLG* and infiltration level of B cells using TIMER2 database. **C** The correlation between *SELPLG* and infiltration level of $CD4^+$ T cells using TIMER2 database. **D** The correlation between *SELPLG* and infiltration level of Macrophage using TIMER2 database. **E** The correlation between *SELPLG* and infiltration level of MDSC using TIMER2 database. **F** The correlation between *SELPLG* and infiltration level of Tregs using TIMER2 database. **G** The correlation between *SELPLG* and infiltration level of indicated immune cells using data from CIBERSOFT database. *$p < 0.05$; **$p < 0.01$; ***$p < 0.001$

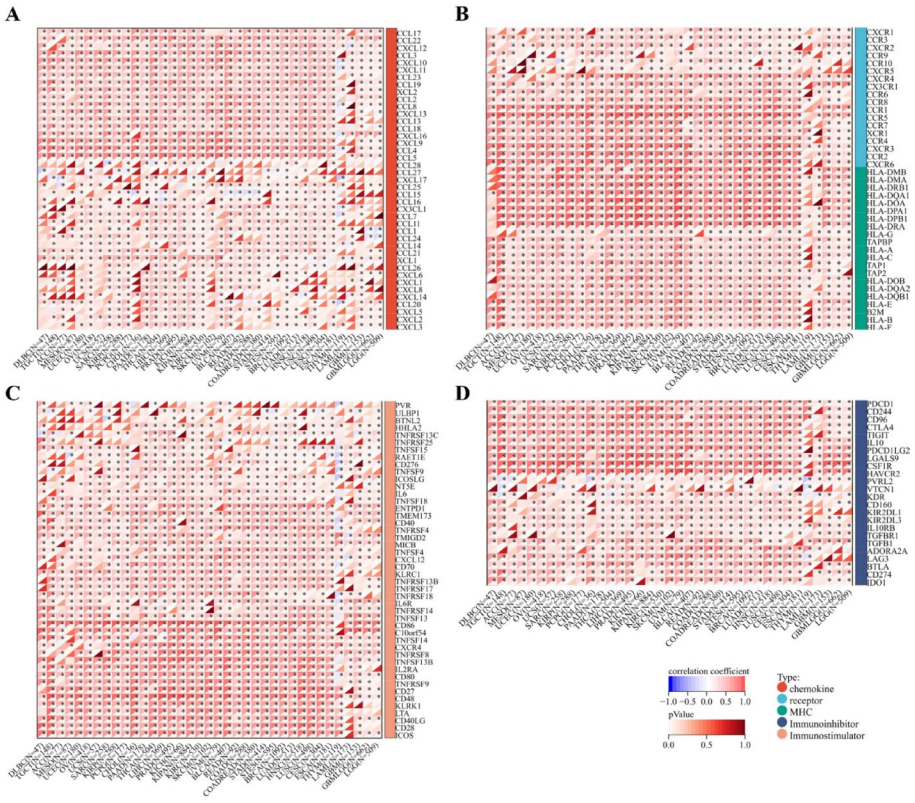

Fig. 8 The correlations between *SELPLG* expression and 122 immunomodulators, including chemokines, chemokine receptors, MHC molecules, immunoinhibitors, and immunostimulators. **A** Heatmap representation of *SELPLG* correlations with chemokine and MHC genes. **B** Heatmap representation of *SELPLG* correlations with chemokine receptor genes. **C***SELPLG*'s correlations with immunoinhibitor genes are depicted in a heatmap, underscoring its interactions with key regulators of immune response modulation. **D** Heatmap representation of *SELPLG* correlations with immunostimulator genes

negative correlations with resting NK cells and memory B cells (Fig. 7G). It is important to note that the observed associations between *SELPLG* expression and immune cell infiltration—particularly involving Tregs and macrophages—are based on correlative data and do not imply direct causality. Although the findings indicate a potential role for *SELPLG* in modulating immune responses, definitive mechanistic evidence remains lacking. Additional experimental validation is necessary to clarify whether *SELPLG* directly influences immune cell infiltration or simply reflects the existing immunological landscape of the tumor microenvironment (TME). Immune cell infiltration patterns varied across tumor types, with minor inconsistencies observed among computational algorithms used for deconvolution. Nonetheless, overarching trends were consistent, reinforcing *SELPLG*'s potential involvement in shaping immune dynamics within the TME.

4.1 Correlation between *SELPLG* expression and Immunomodulatory genes in pan-cancer

To investigate the potential role of *SELPLG* in immunoregulation, pan-cancer correlation analyses were performed. *SELPLG* expression was positively associated with most immunomodulatory genes across cancer types, including chemokines, receptors, and MHC molecules (Fig. 8A–B). Chemokines and their receptors play a fundamental role in immune cell migration and inflammatory responses. The observed positive

correlation between *SELPLG* and genes encoding these molecules suggests that *SELPLG* may enhance immune cell trafficking and positioning, thereby improving immune surveillance and response efficiency (Fig. 8A). Similarly, MHC molecules are essential for antigen presentation and T cell activation. The positive correlation between *SELPLG* and MHC-related genes suggests that *SELPLG* may contribute to the upregulation of MHC expression and function, thereby enhancing the immune system's ability to detect and eliminate tumor cells (Fig. 8B).

Immunoinhibitory and immunostimulatory molecules are key regulators of immune homeostasis. Notably, *SELPLG* exhibited positive correlations with a majority of immune checkpoints, including both inhibitory and stimulatory molecules, across various tumor types (Fig. 8C–D), highlighting *SELPLG*'s role in regulating tumor immunity. These findings suggest that targeting *SELPLG* may modulate immune responses and potentially affect tumor progression (Fig. 8C–D).

In summary, *SELPLG* is intricately linked to immune processes in the tumor microenvironment and may represent a promising target for immunotherapeutic intervention. Modulating its expression could either enhance antitumor immunity or dampen excessive inflammation, depending on the clinical context.

5 Discussion

In this study, we conducted a comprehensive pan-cancer analysis of P-selectin glycoprotein ligand-1 (PSGL-1, encoded by *SELPLG*), uncovering its multifaceted roles in oncogenesis, prognosis, and tumor immunity. By integrating multi-omics datasets and advanced bioinformatics approaches, we identified *SELPLG* as a context-dependent biomarker and potential immunotherapeutic target across various cancer types.

Our results demonstrated that *SELPLG* is significantly upregulated in several carcinomas, such as breast, cholangiocarcinoma, and head and neck cancers, suggesting a role in promoting tumor progression. In contrast, downregulation in lung adenocarcinoma, colon adenocarcinoma, and bladder carcinoma suggests possible tumor-suppressive functions in these contexts. These heterogeneous expression patterns highlight the complexity of *SELPLG*'s role across different tumor types and reinforce the importance of personalized therapeutic strategies. Notably, lower *SELPLG* expression was associated with poorer prognosis in sarcoma (TCGA-SARC), indicating a potentially protective role in mesenchymal-origin tumors. This contrast with its adverse prognostic associations in certain carcinomas underscores the gene's context-specific behavior. Correlations with immune-related pathways and increased infiltration of regulatory T cells and macrophages further support its involvement in modulating the tumor immune microenvironment. Beyond epithelial tumors, *SELPLG* may also contribute to metastasis in mesenchymal-origin tumors such as osteosarcoma. As a key adhesion molecule, *SELPLG* facilitates tumor cell interactions with vascular endothelium, potentially aiding extravasation and metastatic colonization. Osteosarcoma is particularly prone to pulmonary metastasis, and recent studies have highlighted the molecular and cellular mechanisms underlying this process. For instance, a single-cell study revealed that CXCL14 secreted by stem-like osteosarcoma cells activates fibroblasts via the integrin α11β1 axis to establish a lung metastatic niche, promoting tumor invasion and immune suppression [25]. Concurrently, *SELPLG*'s known role in immune cell trafficking and modulation may synergize with such stromal changes to support metastatic outgrowth. Moreover,

a precision nanomedicine strategy for osteosarcoma therapy demonstrated that reprogramming the immune microenvironment can enhance $CD8^+$ T cell infiltration [26], consistent with the observed correlation between *SELPLG* and immune infiltration. Together, these results suggest that *SELPLG* may influence both immune dynamics and metastatic potential via adhesion and stromal signaling mechanisms.

In addition, *SELPLG*'s mutational landscape revealed frequent missense mutations across multiple tumor types, which may affect its function and contribute to tumor progression. These mutations could serve as potential biomarkers or therapeutic targets in genetically defined patient subsets. Expression of *SELPLG* was positively associated with key immune populations-including $CD8^+$ T cells, Tregs, and macrophages-and with immune-regulatory pathways such as antigen presentation, T cell activation, and cytokine signaling, indicating a broader role in shaping the tumor immune microenvironment. Although these findings suggest an immunomodulatory role, causality requires further experimental validation.

Recent studies have identified PSGL-1 (encoded by *SELPLG*) as an emerging immune checkpoint molecule. Antibody-mediated blockade has been shown to restore $CD8^+$ T cell function and inhibit tumor progression. In line with this, *SELPLG* expression was enriched in lymphoid and myeloid lineages, particularly macrophages. CIBERSORT analysis further indicated positive correlation with both M1 and M2 tumor-associated macrophages (TAMs), suggesting a role in modulating immune cell polarization within the tumor microenvironment [27–29]. Given the established immunosuppressive role of M2 TAMs—mediated by cytokines such as IL-10 and TGF-β [30], the association between *SELPLG* and macrophage infiltration may reflect a potential immunosuppressive axis [27, 31]. Notably, PSGL-1 blockade has been reported to reduce M2 markers and promote macrophage repolarization [32], although further validation in solid tumors is still needed. Beyond macrophages, PSGL-1 influences T cell exhaustion and tolerance. *SELPLG*-deficient mice display enhanced effector T cell responses are observed, accompanied by autoimmune features, reflecting its dual function in immune regulation and homeostasis [33]. In dendritic cells, PSGL-1 signaling promotes tolerogenic phenotypes and Treg differentiation [17], while interaction with VISTA under acidic conditions contributes to T cell suppression [34, 35]. These diverse interactions underscore *SELPLG*'s involvement in immune evasion, though its signaling remains incompletely understood due to the absence of canonical intracellular motifs [36]. These results suggest that *SELPLG* may contribute to immune modulation within the TME, but further research is needed to clarify whether it actively regulates immune responses or simply reflects immune activity [15].

In summary, the pan-cancer analysis highlights *SELPLG* as a context-dependent biomarker associated with immune cell infiltration and immunomodulatory signaling within the tumor microenvironment. Its correlations with immune checkpoints and effector cell populations suggest potential roles in immune evasion and tumor progression. While these associations provide a foundation for understanding *SELPLG*'s immunological relevance, additional experimental studies are essential to elucidate its mechanistic function and therapeutic applicability. A deeper investigation of its expression, mutations, and functional signaling may ultimately inform the development of *SELPLG*-targeted strategies in cancer immunotherapy.

Supplementary Information

The online version contains supplementary material available at https://doi.org/10.1007/s12672-025-02934-0.

Supplementary Material 1

Acknowledgements

We thank the Foundation of Henan Province for support. The results shown here are in whole or part based upon data generated by the TCGA Research Network: https://www.cancer.gov/tcga.

Author contributions

R.S., L.R., B.L., Y.T., W.G., S.J., and W.Z. contributed to the conception and design of the study. R.S. and L.R. performed data collection and analysis. B.L., Y.T., and W.G. contributed to prepared figures. S.J. and W.Z. drafted the manuscript. All authors critically reviewed and approved the final manuscript.

Funding

This work was supported by the Doctoral Scientific Research Start-up Foundation of Luohe Medical College (No. 2022-DF-02), Science and Technology Research Project of Henan Provincial Department of Science and Technology (No. 232102310216, 252102310393), Key Research Projects of Higher Education Institutions in Henan Province (No. 24B310002), Luohe Medical College Science and Technology Innovation Project (No. 2023ZD01, KJCX202401), Natural Science Foundation of Henan Province (No. 252300420627).

Data availability

The data supporting this study was obtained from the TCGA (https://www.cancer.gov/tcga) database.

Declarations

Consent for publication

All authors declare that they agree to submit the article for publication.

Competing interests

The authors declare no competing interests.

Received: 9 October 2024 / Accepted: 6 June 2025

Published online: 12 June 2025

References

1. Budimir N, Thomas GD, Dolina JS, Salek-Ardakani S. Reversing t-cell exhaustion in cancer: lessons learned from pd-1/pd-l1 immune checkpoint Blockade. Cancer Immunol Res. 2022;10:146–53.
2. DeRogatis JM, Viramontes KM, Neubert EN, Tinoco R. Psgl-1 immune checkpoint Inhibition for cd4(+) t cell cancer immunotherapy. Front Immunol. 2021;12:636238.
3. Heidemann F, Schildt A, Schmid K, Bruns OT, Riecken K, Jung C, et al. Selectins mediate small cell lung cancer systemic metastasis. PLoS ONE. 2014;9:e92327.
4. Azab AK, Quang P, Azab F, Pitsillides C, Thompson B, Chonghaile T, et al. P-selectin glycoprotein ligand regulates the interaction of multiple myeloma cells with the bone marrow microenvironment. Blood. 2012;119:1468–78.
5. Dimitroff CJ, Descheny L, Trujillo N, Kim R, Nguyen V, Huang W, et al. Identification of leukocyte e-selectin ligands, p-selectin glycoprotein ligand-1 and e-selectin ligand-1, on human metastatic prostate tumor cells. Cancer Res. 2005;65:5750–60.
6. Gong L, Cai Y, Zhou X, Yang H. Activated platelets interact with lung cancer cells through p-selectin glycoprotein ligand-1. Pathol Oncol Res. 2012;18:989–96.
7. Borsig L. The role of platelet activation in tumor metastasis. Expert Rev Anticancer Ther. 2008;8:1247–55.
8. Zheng Y, Yang J, Qian J, Qiu P, Hanabuchi S, Lu Y, et al. Psgl-1/selectin and icam-1/cd18 interactions are involved in macrophage-induced drug resistance in myeloma. Leukemia. 2013;27:702–10.
9. Muz B, Azab F, de la Puente P, Rollins S, Alvarez R, Kawar Z, et al. Inhibition of p-selectin and psgl-1 using humanized monoclonal antibodies increases the sensitivity of multiple myeloma cells to bortezomib. Biomed Res Int. 2015;2015:417586.
10. Erbani J, Tay J, Barbier V, Levesque JP, Winkler IG. Acute myeloid leukemia chemo-resistance is mediated by e-selectin receptor cd162 in bone marrow niches. Front Cell Dev Biol. 2020;8:668.
11. Perez-Frias A, Gonzalez-Tajuelo R, Nunez-Andrade N, Tejedor R, Garcia-Blanco MJ, Vicente-Rabaneda E, et al. Development of an autoimmune syndrome affecting the skin and internal organs in p-selectin glycoprotein ligand 1 leukocyte receptor-deficient mice. Arthritis Rheumatol. 2014;66:3178–89.
12. Angiari S, Rossi B, Piccio L, Zinselmeyer BH, Budui S, Zenaro E, et al. Regulatory t cells suppress the late phase of the immune response in lymph nodes through p-selectin glycoprotein ligand-1. J Immunol. 2013;191:5489–500.
13. He X, Schoeb TR, Panoskaltsis-Mortari A, Zinn KR, Kesterson RA, Zhang J, et al. Deficiency of p-selectin or p-selectin glycoprotein ligand-1 leads to accelerated development of glomerulonephritis and increased expression of Cc chemokine ligand 2 in lupus-prone mice. J Immunol. 2006;177:8748–56.
14. Nunez-Andrade N, Lamana A, Sancho D, Gisbert JP, Gonzalez-Amaro R, Sanchez-Madrid F, et al. P-selectin glycoprotein ligand-1 modulates immune inflammatory responses in the enteric lamina propria. J Pathol. 2011;224:212–21.
15. Tinoco R, Carrette F, Barraza ML, Otero DC, Magaña J, Bosenberg MW et al. Psgl-1 is an immune checkpoint regulator that promotes t cell exhaustion. Immunity. 2016;44:1190 – 203.
16. DeRogatis JM, Viramontes KM, Neubert EN, Henriquez ML, Guerrero-Juarez CF, Tinoco R. Targeting the psgl-1 immune checkpoint promotes immunity to pd-1-resistant melanoma. Cancer Immunol Res. 2022;10:612–25.

17. Urzainqui A, Martinez del Hoyo G, Lamana A, de la Fuente H, Barreiro O, Olazabal IM, et al. Functional role of p-selectin glycoprotein ligand 1/p-selectin interaction in the generation of tolerogenic dendritic cells. J Immunol. 2007;179:7457–65.
18. Spertini C, Baisse B, Spertini O. Ezrin-radixin-moesin-binding sequence of psgl-1 glycoprotein regulates leukocyte rolling on selectins and activation of extracellular signal-regulated kinases. J Biol Chem. 2012;287:10693–702.
19. Urzainqui A, Serrador JM, Viedma F, Yanez-Mo M, Rodriguez A, Corbi AL, et al. Itam-based interaction of erm proteins with Syk mediates signaling by the leukocyte adhesion receptor psgl-1. Immunity. 2002;17:401–12.
20. Bi F, Chen Y, Yang Q. Significance of tumor mutation burden combined with immune infiltrates in the progression and prognosis of ovarian cancer. Cancer Cell Int. 2020;20:373.
21. Mayakonda A, Lin DC, Assenov Y, Plass C, Koeffler HP. Maftools: efficient and comprehensive analysis of somatic variants in cancer. Genome Res. 2018;28:1747–56.
22. Liu J, Lichtenberg T, Hoadley KA, Poisson LM, Lazar AJ, Cherniack AD et al. An integrated tcga pan-cancer clinical data resource to drive high-quality survival outcome analytics. Cell. 2018;173:400 – 16 e11.
23. Thorsson V, Gibbs DL, Brown SD, Wolf D, Bortone DS, Ou Yang TH et al. The immune landscape of cancer. Immunity. 2018;48:812 – 30 e14.
24. Liu Z, Liu L, Weng S, Xu H, Xing Z, Ren Y et al. Best: A web application for comprehensive biomarker exploration on large-scale data in solid tumors. Journal of Big Data. 2023;10:165.
25. Xu Y, Deng C, Chen H, Song Y, Xu H, Song G, et al. Osteosarcoma cells secrete cxcl14 that activates integrin α11β1 on fibroblasts to form a lung metastatic niche. Cancer Res. 2024;84:994–1012.
26. Luo T, Fan Z, Zeng A, Wang A, Pan Y, Xu Y, et al. Biomimetic targeted co-delivery system engineered from genomic insights for precision treatment of osteosarcoma. Adv Sci (Weinh). 2025;12:e2410427.
27. Petty AJ, Owen DH, Yang Y, Huang X. Targeting tumor-associated macrophages in cancer immunotherapy. Cancers (Basel) 2021;13.
28. Zhu S, Yi M, Wu Y, Dong B, Wu K. Roles of tumor-associated macrophages in tumor progression: implications on therapeutic strategies. Exp Hematol Oncol. 2021;10:60.
29. Sica A, Schioppa T, Mantovani A, Allavena P. Tumour-associated macrophages are a distinct m2 polarised population promoting tumour progression: potential targets of anti-cancer therapy. Eur J Cancer. 2006;42:717–27.
30. Noy R, Pollard JW. Tumor-associated macrophages: from mechanisms to therapy. Immunity. 2014;41:49–61.
31. Zhang M, Hutter G, Kahn SA, Azad TD, Gholamin S, Xu CY, et al. Anti-cd47 treatment stimulates phagocytosis of glioblastoma by m1 and m2 polarized macrophages and promotes m1 polarized macrophages in vivo. PLoS ONE. 2016;11:e0153550.
32. Kauffman K, Manfra D, Nowakowska D, Zafari M, Nguyen PA, Phennicie R, et al. Psgl-1 Blockade induces classical activation of human tumor-associated macrophages. Cancer Res Commun. 2023;3:2182–94.
33. Tinoco R, Otero DC, Takahashi AA, Bradley LM. Psgl-1: A new player in the immune checkpoint landscape. Trends Immunol. 2017;38:323–35.
34. Johnston RJ, Su LJ, Pinckney J, Critton D, Boyer E, Krishnakumar A, et al. Vista is an acidic ph-selective ligand for psgl-1. Nature. 2019;574:565–70.
35. Olbromski M, Mrozowska M, Piotrowska A, Smolarz B, Romanowicz H. The vista/vsig3/psgl-1 axis: crosstalk between immune effector cells and cancer cells in invasive ductal breast carcinoma. Cancer Immunol Immunother. 2024;73:136.
36. Bernimoulin MP, Zeng XL, Abbal C, Giraud S, Martinez M, Michielin O, et al. Molecular basis of leukocyte rolling on psgl-1. Predominant role of core-2 o-glycans and of tyrosine sulfate residue 51. J Biol Chem. 2003;278:37–47.

Publisher's note